

Optimally Designed Digitally-Doped Mn:GaAs

J. L. Xu¹ and M. van Schilfgaarde¹

¹*Department of Chemical and Materials Engineering, Arizona State University, Tempe, AZ, 85287**
(Dated: November 11, 2018)

We use the *ab initio* local-density approximation (LDA) to study of exchange interactions and T_c of $\text{Ga}_{1-x}\text{Mn}_x\text{As}$ grown in digitally doped structures. We analyze the crystallographic dependence of exchange interactions predicted by the LDA in terms of the Mn t_2 and e levels, and explain the origin of the antiferromagnetic contribution to the total exchange interactions. We exploit this dependence and consider δ -doping in specific orientations where the antiferromagnetic interactions are minimized, to optimize T_c of the system. By including hole doping with the addition of Be in the GaAs host digitally doped $\text{Ga}_{1-x}\text{Mn}_x\text{As}$ is predicted to be significantly above room temperature.

PACS numbers: 75.50.Pp, 75.30.Et, 71.15.Mb

Spintronics-based materials have attracted a lot of interest recently^{1,2}. By introducing spin as a degree of freedom existing technologies can be improved, e.g. smaller devices³

that consume less electricity, and are more powerful for certain types of computations as compared to present charge-based systems. A key point is that the magnetism be carrier-mediated, i.e. the magnetic state can be manipulated by electrical or optical means. Dilute magnetic semiconductors (DMS), i.e. semiconductors doped with low concentrations of magnetic impurities Mn, Cr, or Co, especially Mn doped GaAs, are generally thought to be good candidates to meet the requirements for spintronics applications. A central issue that has impeded the spintronics field is the lack of a (demonstrably) carrier-mediated ferromagnetic semiconductor with critical temperature T_c above room temperature.

In $\text{Ga}_{1-x}\text{Mn}_x\text{As}$, Mn ions (approximately) randomly occupy the Ga sites and act as both spin providers ($S=5/2$) and acceptors. Because ferromagnetic coupling between local ions is mediated by carriers (holes in $\text{Ga}_{1-x}\text{Mn}_x\text{As}$), the doping concentration is believed to be a crucial factor which determines the ferromagnetic properties of DMS.

Traditionally, people use molecular beam epitaxy (MBE) methods to grow DMS thin films with magnetic elements randomly doped into the host semiconductors^{1,4,5}. However, this preparation process always suffers of the low solubility of the magnetic elements, and the tendency of Mn to form interstitials deleterious to the magnetism. Although annealing significantly improves the quality of the samples, optimized Curie temperatures (T_c) for these random alloys are below 200K⁶, well below requirements for room temperature applications. Although T_c is predicted to be enhanced when the material is co-doped with acceptors, attempts to do this with holes has not been successful.⁷

An alternative to a random alloy, δ -doping of Mn in a GaAs host has also been attempted with some success^{7,8,9,10}. A very thin MnAs layer is periodically doped in a GaAs epitaxial layer, produce high Mn doping concentration in a few (typically 2 to 3) GaAs monolayers (ML). Because the Mn-derived impurity band sits slightly

above the GaAs valence band, and is approximately localized within the Mn layer, the holes are thus confined, which according to simple models should increase T_c .¹¹

In this paper, we use a first-principles linear response approach based on the local-density approximation (LDA), to study ferromagnetism in δ -doped $\text{Ga}_{1-x}\text{Mn}_x\text{As}$, and contrast it to the random alloy. We show the following, and explain each point qualitatively from the electronic structure of Mn d levels: (i) The magnetic exchange interactions have a strong crystallographic and concentration dependence. As a result: (ii) There is an optimal Mn concentration within the δ -layer; (iii) There is an optimal δ -layer thickness; (iv) p -type doping (Be in GaAs) in the substrate can increase T_c of the system by a large amount, bringing it well above room temperature.

We adopt a linear-response approach¹² valid in the rigid-spin and long-wave approximation¹³, in which the change in energy from noncollinear spin configurations is mapped onto a Heisenberg form $H = -\sum_{RR'} J_{RR'} \hat{e}_R \cdot \hat{e}_{R'}$.

In multiple-scattering theory the $J_{RR'}$ are computed from the scaled susceptibility¹²:

$$J_{RR'} = \frac{1}{\pi} \text{Im} \int_{-\infty}^{\epsilon_F} \sum_{LL'} d\epsilon \{ \delta P_{RL} T_{RL,R'L'} T_{R'L',RL} \delta P_{R'L'} \} \quad (1)$$

The notation and computational approach is based on the Atomic Spheres approximation and is described in detail in Ref. 14. $T_{RL,R'L'}$ is related to the Green's function and δP_{RL} is related to the exchange splitting. L is a compound index referring to the l and m quantum numbers of the orbitals at a site.

Because of the large Mn local moment, the approximations are expected to be reasonable. A previous paper using the same approach presents results for random alloys¹⁵. The finite temperature magnetization $M(T)$ is obtained from the Heisenberg form assuming classical spins. The cluster variation method (CVM)¹⁶ adapted to the heisenberg hamiltonian was used to obtain T_c ; it was shown in Ref. 15 that the (CVM) does a rather good job of estimating T_c in random DMS alloys, and is expected to be comparably accurate here.

All the calculations are performed using supercells with periodic boundary conditions. The supercell we use includes 8ML in the [001] direction. We set the thickness of Mn layer to be 1 or 2 ML, which is comparable with the experiment setup. The inter-layer distance is chosen to be 6 ML which is an optimized value based on both speed and accuracy considerations. Checks show that further increase of the interlayer distance does not significantly affect the exchange interactions T_c . The lateral scale of the layers are chosen based on Mn concentration simulated. Both ordered and Special Quasi-Random Structures (SQS)¹⁷ are used to simulate Mn doping inside the δ layer.

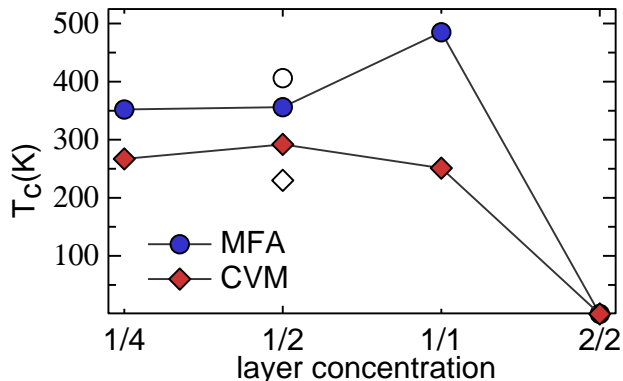


FIG. 1: Dependence of T_c on Mn concentration inside a superlattice consisting of a 1-2 ML thick δ -layer of Mn, sandwiched by a 6 ML thick GaAs layer. Mn are taken to form an ordered structure within the δ -layer. The x axis refers to the fraction of Ga atoms that are replaced by Mn in the layer considered. In the “ m/n ” label along x axis, m represents the number of ML in the Mn doped layer, and n is the total number of cation sites in the doped layer. Circles show mean-field results for comparison. The 2/2 system is predicted to be a frustrated spin glass; this is reflected in the figure by assigning $T_c=0$. Open diamond (circle) : T_c for an SQS structure spread over 1ML at 50% concentration calculated within the CVM (MFA).

We first investigate a series of ordered δ -layers varying concentration within the layer for 1-2 ML superlattices. Fig 1 shows the calculated T_c for the Mn concentration in the δ -layer ranging between 1/4 and 1.¹⁸

For bulk random alloys¹⁵, the disorder in the Mn site positions rather strongly affects exchange interactions and reduces T_c . In the bulk $\text{Ga}_{1-x}\text{Mn}_x\text{As}$ alloy, the predicted optimum T_c was found to be $\sim 300\text{K}$ at $x=12\%$. Fig. 1 compares an ordered to a disordered configuration of Mn within the δ -layer in the 1/2 filling case (Mn position in the ML were simulated by an SQS structure). It is seen that the effect of disorder is to reduce T_c slightly, just as in the bulk random alloy. (Note that mean-field theory incorrectly predicts T_c increases with disorder, as was also found in the bulk alloy.)

Notably, the optimum T_c for the δ -layer case occurs near 50% filling in a single ML and the optimum T_c is near that predicted for the bulk case ($\sim 300\text{K}$ at $x=12\%$).

Most of this effect can be traced to the strong crystallographic dependence of the magnetic exchange interactions. This can be seen by considering exchange interactions $J_{RR'}$ in $\text{Ga}_{1-x}\text{Mn}_x\text{As}$ compounds of high Mn concentration (Fig. 3). While there is some variation between compounds, there is a tendency for the $J_{RR'}$ to be *weak or even* antiferromagnetic along the [001] axis, but to be *more strongly* ferromagnetic along the [110] axis. A similar result is found for the dilute random alloys¹⁵. The origin of the strong crystallographic dependence can, at least in part, be explained in terms of the orbital character of the Mn d orbitals of t_2 and e symmetry. Mn impurities in GaAs form a “dangling bond hybrid” level¹⁹ of t_2 symmetry which sits $\sim 0.1\text{eV}$ above the valence band maximum, and is an admixture of the Mn d levels of t_2 symmetry (xy , yz , and xz) and effective-mass like states derived from the top of the host valence band. Below the valence band top sit Mn d orbitals of e symmetry ($3z^2-r^2$ and x^2-y^2), which hybridize less strongly with the environment than the t_2 orbitals. As is well known, the e states are filled, while the three t_2 states are partially filled with 2 electrons. (Mn, with 5 d electrons and 2 sp electrons, substitutes for Ga, with 3 sp electrons. Thus Mn contributes 5 d electrons and a hole.)

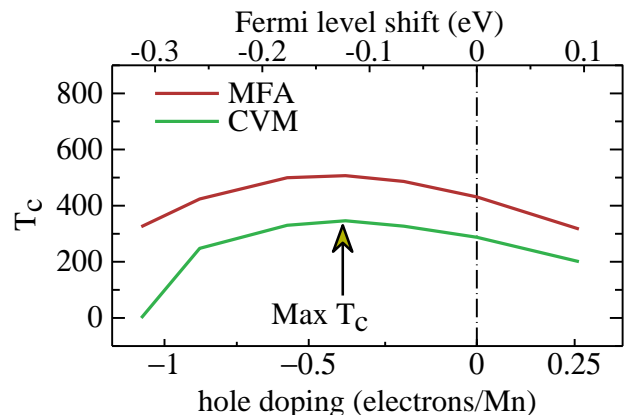
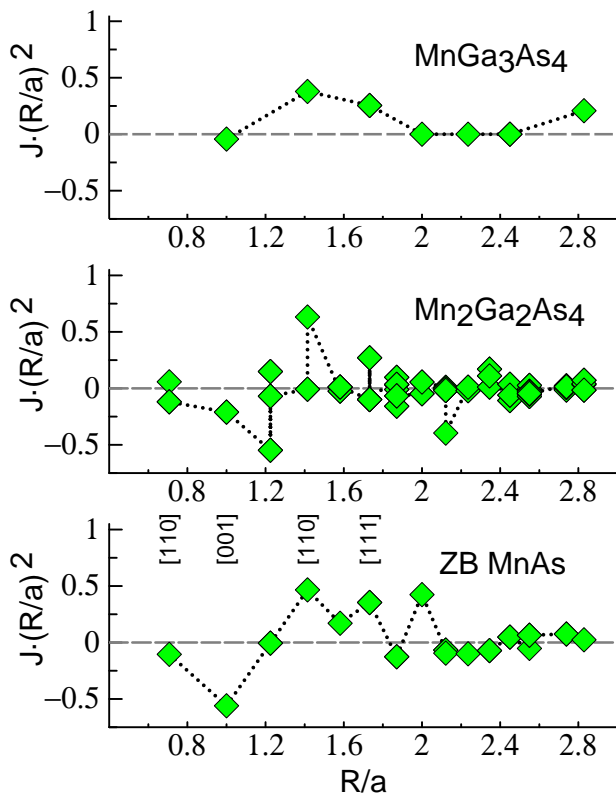


FIG. 2: Dependence of T_c on the Fermi level shift and excess hole concentration in a bulk SQS $\text{Ga}_{92}\text{Mn}_8\text{As}_{100}$ alloy. $E_F = 0$ corresponds to the usual charge-neutral case.

While there is some disagreement as to whether the exchange is best described by an RKKY-like picture²⁰ or a double exchange picture²¹, it is generally agreed that FM in $\text{Ga}_{1-x}\text{Mn}_x\text{As}$ derives from the partial filling of the t_2 level. According to the Zener-Anderson-Hasegawa model^{22,23} of double exchange/superexchange, exchange interactions between sites depend on the filling. At half filling the interactions are ferromagnetic, while filled levels couple antiferromagnetically. To the extent that this model is a valid description of FM in the $\text{Ga}_{1-x}\text{Mn}_x\text{As}$ system, the exchange interactions should be maximally FM when the t_2 level is half full. This is apparently a reasonable description of the LDA exchange interactions, as Fig. 2 shows. Exchange parameters $J_{RR'}$ were computed in a bulk SQS-100 structure at 8% Mn concentration, as



Structure	t_2	e	sp	total
L1 ₂	470	-104	16	382
SQS-4	102	-250	76	-71
ZB	-6	-206	78	-134

FIG. 3: Scaled exchange interactions $J_{RR'} \times R^2$ as a function of separation $R = |\mathbf{R} - \mathbf{R}'|$. R is in units of the lattice constant a . (top) MnGa_3As_4 in the $L1_2$ structure; (middle) the SQS-4 $\text{Mn}_2\text{Ga}_2\text{As}_4$; (bottom) MnAs in the ZB phase. In the SQS-4 structure a given R be found in different environments, a rather strong dispersion in $J_{RR'}$ for a particular R is evident. The Table shows resolution of T_c^{MFA} into contributions from the Mn t_2 , e and sp orbitals.

a function of Fermi level (thus altering the filling of the t_2 level), i.e. additional holes are modeled by simple Fermi level shifts. The $J_{RR'}$ and T_c are maximal when the t_2 level contains approximately $3/2$ electrons.

If this applies to both the t_2 and e levels, the t_2 level should contribute a FM exchange, while the e level should contribute a competing AFM exchange. To see to what extent this model describes the LDA exchange we resolve the mean-field estimate for T_c into separate l and m contributions, that is

$$\begin{aligned}
 T_c^{\text{MFA}} &= \sum_L T_{c,L}^{\text{MFA}} \\
 T_{c,L}^{\text{MFA}} &= \frac{2}{3} \sum_{RR'L'} J_{RL'R'L'} \quad (2)
 \end{aligned}$$

where $J_{RL'R'L'}$ is identical to Eq. (1) but with the sum

over LL' suppressed. Three compounds with high Mn concentration were studied: MnGa_3As_4 in the $L1_2$ structure, a four-atom SQS alloy $\text{Mn}_2\text{Ga}_2\text{As}_4$, and MnAs in the ZB phase. Data shown in Fig. 3 largely verifies this picture. The table in Fig. 3 shows the e levels consistently contribute antiferromagnetically. FM contributions from t_2 level decrease with increasing Mn concentration. In the high concentration limit (ZB MnAs) the picture of a t_2 derived impurity band is rather far removed from reality. Fig. 3 also shows site-resolved $J_{RR'}$. It shows that $J_{RR'}$ when R points along $[110]$ tend to be FM, while those pointing along $[001]$ tend to be AFM. This tendency is compatible with symmetry of the t_2 orbitals, which point in the $[110]$ directions and are FM coupled, while the e orbitals point along the $[001]$ are *weak or even* AFM coupled. Thus it seems that the LDA exchange interactions are rather strongly dependent on symmetry of the Mn orbitals rather than largely being a function of the Fermi surface, as RKKY-like models suppose²⁰.

The orientation dependence of J has been studied previously by a number of authors, mostly in the dilute case where the Mn doping concentration is $< 10\%$ ^{24,25,26,27,28}. One approach estimates J from various FM-AFM configurations^{24,25,26,29}. However, such calculations are predicated on the assumption that large-angle rotations can map to a Heisenberg model (a perturbation theory valid for small rotations). More importantly, this is approach is problematic especially for dilute case, because many J 's are required. The longer-ranged J s are important to describe T_c , where percolation is important¹⁵. The more rigorously based linear-response technique²⁷ explicitly calculates energy changes for small angle rotations. Many J s are calculated at once; and the range extends far beyond the unit cell. In any case, none of the preceding calculations yield AFM coupling in the $[001]$ direction, because the competing antiferromagnetic interactions are much stronger at high concentrations²⁹, at least in the LDA. In the dilute case, we obtain both FM and AFM exchange coupling for $[001]$ direction, which when averaged yields a small net coupling, similar to a CPA linear-response calculation²⁷. However, for high Mn doping in the δ -doped case studied here, AFM becomes increasingly dominant along $[001]$.

The crystallographic dependence of $J_{RR'}$, and the reduction of $J_{RR'}$ with Mn concentration, help to explain why T_c is maximal for partial fillings of the δ layer (Fig. 1), and also suggest that T_c will be optimal for a rather small δ layer thickness. To test this, we compute T_c varying the number δ layers. We fix the total thickness of the supercell as 8ML and change the thickness of δ -layer up to 8ML (corresponding to the bulk case). Each layer contains 50% Mn and 50% Ga (the 1-layer case corresponds to the “1/2” point in Fig. 1). Data is shown in Fig. 4. T_c is optimal at 2ML then decreases above that. (For thicknesses > 2 ML only T_c^{MFA} is shown CVM predicts a spin glass).

We now turn to the question: can T_c be increased by co-doping to add holes? We can mimic addition of holes

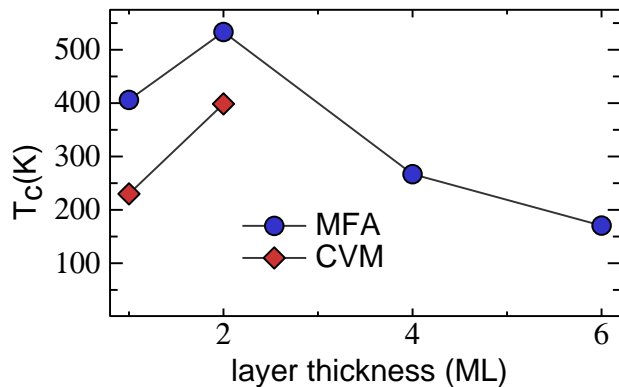


FIG. 4: Dependence of T_c on the δ -layer thickness for an average Mn concentration of 50% per layer. Circles show mean-field results for comparison.

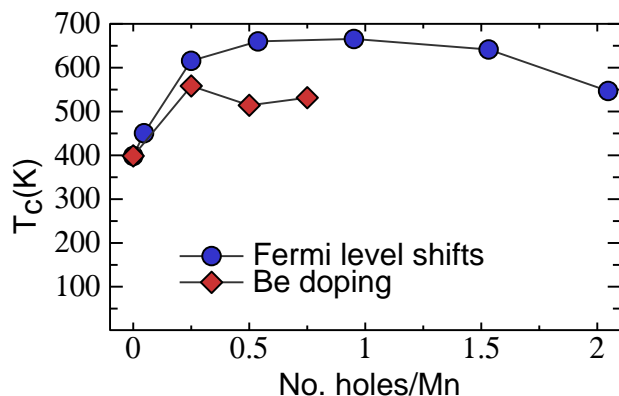


FIG. 5: Dependence of T_c on excess hole concentration for a 2ML δ -doped MnGaAs structure, with the δ layer containing 50% Mn, as calculated by the CVM. Hole doping is modeled through artificial Fermi level shifts, or induced through the addition of Be in GaAs layers adjacent to the δ layer.

by Fermi level shifts (as before); alternatively we can dope the GaAs layer with an acceptor such as Be. In Ref. 10, δ -doped MnGaAs were grown in this way. Extra holes were supplied to the δ -layer by doping Be in the GaAs near (but not in) the δ -layer, to prevent compensating donors such as Mn interstitials from forming in the δ -layer.

In Fig. 5, the dependence of T_c on the number of extra holes is presented. T_c increases markedly by the addition of $\sim 1/2$ hole/Mn atom. Higher hole concentrations do not further increase T_c (as in the random alloy). The difference between Fermi level shifts and using actual dopants can be explained in that the latter contains electrostatic shifts as a result of charge transfer from the Be dopants to the Mn layers, thus reducing hole confinement in the δ layer. This confirms the experimental results for δ layer and also suggest a much higher T_c for defect free samples compared with the best T_c recorded to date.

In conclusion, we demonstrate a strong crystallographic dependence of magnetic exchange interactions in $\text{Ga}_{1-x}\text{Mn}_x\text{As}$, and show that it can be exploited in δ -doped Mn:GaAs structures to optimize T_c . We determine the size and concentration of δ -layers, and hole concentration that are predicted to result in an optimal T_c . Under optimal conditions (which entails superlattices to be grown sufficiently defect-free) T_c is predicted to be well above room temperature.

This work was supported by ONR contract N00014-02-1-1025.

-
- * Mark.vanSchilfgaarde@asu.edu
- ¹ H. Ohno, et al., Applied Physics Letters **69**, 363 (1996).
 - ² Y. Ohno, et al., Nature **402**, 790 (1999).
 - ³ S. Datta and B. Das, Appl. Phys. Lett. **56**, 665 (1990).
 - ⁴ D. Chiba, K. Takamura, F. Matsukura, and H. Ohno, Appl. Phys. Lett. **82**, 3020 (2003).
 - ⁵ K. C. Ku, et al., Appl. Phys. Lett. **82**, 2302 (2003).
 - ⁶ K. W. Edmonds, et al., Phys. Rev. Lett. **92**, 037201 (2004).
 - ⁷ T. Wojtowicz, et al., Appl. Phys. Lett. **83**, 4220 (2003).
 - ⁸ R. K. Kawakami, et al., Appl. Phys. Lett. **77**, 2379 (2000).
 - ⁹ A. M. Nazmul, S. Sugahara, and M. Tanaka, Phys. Rev. B **67**, 241308 (2003).
 - ¹⁰ A. M. Nazmul, T. Amemiya, Y. Shuto, S. Sugahara, and M. Tanaka, Phys. Rev. Lett. **95**, 017201 (2005).
 - ¹¹ J. Fernández-Rossier and L. J. Sham, Phys. Rev. B **64**, 235323 (2001).
 - ¹² A. I. Liechtenstein, M. I. Katsnelson, V. P. Antropov, and V. A. Gubanov, J. Magn. Magn. Mater. **67**, 65 (1987).
 - ¹³ V. Antropov, J. Magn. Magn. Mater. **262**, L192 (2003).
 - ¹⁴ M. van Schilfgaarde and V. P. Antropov, J. Appl. Phys. **85**, 4827 (1999).
 - ¹⁵ J. L. Xu, M. van Schilfgaarde, and G. D. Samolyuk, Phys. Rev. Lett. **94**, 097201 (2005).
 - ¹⁶ R. Kikuchi, Phys. Rev. **81**, 988 (1951).
 - ¹⁷ A. Zunger, S.-H. Wei, L. G. Ferreira, and J. E. Bernard, Phys. Rev. Lett. **65**, 353 (1990).
 - ¹⁸ It was recently shown by an analysis of the 2D Heisenberg ferromagnet within the RPA, that even though the vanilla Heisenberg hamiltonian orders at 0K³⁰, a small amount anisotropy acts as a “trigger” to stabilize T_c (T_c depends weakly on the anisotropy when it is small)³¹. We compute the anisotropy for some 1 ML cases, and find that it depends rather sensitively on the detailed configuration of atoms in the monolayer, ranging from 0.3 to 20 meV. It sufficient to stabilize the FM in this 2D structure, so we can reasonably neglect it in these calculations.
 - ¹⁹ P. Mahadevan and A. Zunger, Phys. Rev. B **69**, 115211 (2004).
 - ²⁰ T. Dietl, H. Ohno, F. Matsukura, J. Cibert, and D. Fermand, Science **287**, 1019 (2002).

- ²¹ H. Akai, Phys. Rev. Lett. **81**, 3002 (1998).
- ²² C. Zener, Phys. Rev. **82**, 403 (1951).
- ²³ P. W. Anderson and H. Hasegawa, Phys. Rev. **100**, 675 (1955).
- ²⁴ Y.-J. Zhao, P. Mahadevan, and A. Zunger, Appl. Phys. Lett. **84**, 3753 (2004).
- ²⁵ P. Mahadevan and A. Zunger, Appl. Phys. Lett. **85**, 2860 (2004).
- ²⁶ A. J. R. da Silva, A. Fazzio, R. R. dos Santos, and L. E. Oliveira, J. Phys.: Condens. Matter. **16**, 8243 (2004).
- ²⁷ L. Bergqvist, et al., Phys. Rev. B **72**, 195210 (2005).
- ²⁸ J. Kudrnovský, et al., Phys. Rev. B **69**, 115208 (2004)
- ²⁹ M. van Schilfgaarde and O. Mryasov, Phys. Rev. B **63**, 233205 (2001).
- ³⁰ N. D. Mermin and H. Wagner, Phys. Rev. Lett. **17**, 1133 (1966).
- ³¹ L. M. Sandratskii, E. Şaşıoğlu, and P. Bruno, Physical Review B **73**, 014430 (2006).